

1

2 Colitis is associated with loss of LHPP and up-regulation of
3 histidine phosphorylation in intestinal epithelial cells

4

5

6 Markus Linder^{1,2}, Dritan Liko¹, Venkatesh Kancharla³, Salvatore Piscuoglio^{3,4} and
7 Michael N. Hall^{1,5}

8

9 ¹ *Biozentrum, University of Basel, CH-4056 Basel, Switzerland*

10 ² *Current address: Roche Pharma Research and Early Development, Roche Innovation
11 Center Basel, F. Hoffmann-La Roche Ltd., CH-4070 Basel, Switzerland*

12 ³ *Institute of Medical Genetics and Pathology, University Hospital Basel, CH-4031 Basel,
13 Switzerland*

14 ⁴ *Visceral Surgery and Precision Medicine research laboratory, Department of Biomedicine,
15 University of Basel, CH-4031 Basel, Switzerland*

16 ⁵ *Corresponding author, m.hall@unibas.ch*

17

18 **Keywords**

19 Histidine phosphorylation, LHPP, inflammatory bowel disease

20

21 **This PDF file includes:**

22 Main Text

23 Figures 1 and 2

24 **Abstract**

25 Protein histidine phosphorylation (pHis) is a posttranslational modification involved in
26 cell cycle regulation, ion channel activity and phagocytosis (1). Using novel
27 monoclonal antibodies to detect pHis (2), we recently reported that loss of the
28 histidine phosphatase LHPP results in elevated pHis levels in hepatocellular
29 carcinoma (3). Here, we show that intestinal inflammation correlates with loss of
30 LHPP, in DSS-treated mice and in inflammatory bowel disease (IBD) patients.
31 Increased histidine phosphorylation was observed in intestinal epithelial cells (IECs),
32 as determined by pHis immunofluorescence staining of colon samples from a colitis
33 mouse model. However, ablation of *Lhpp* did not cause increased pHis or promote
34 intestinal inflammation in physiological conditions or after DSS treatment. Our
35 observations suggest that increased histidine phosphorylation plays a role in colitis,
36 but loss of LHPP is not sufficient to increase pHis or to cause inflammation in the
37 intestine.

38

39 **Introduction**

40 Protein histidine phosphorylation, a poorly characterized posttranslational
41 modification, refers to the the addition of a phosphate group to the imidazole ring of
42 histidine via a heat and acid labile phosphoramidate (P-N) bond. Both nitrogens in
43 the histidine imidazole ring can be phosphorylated resulting in the formation of two
44 isomers: 1-phosphohistidine (1-pHis) and 3-phosphohistidine (3-pHis). So far, three
45 mammalian histidine phosphatases (LHPP, PGAM5 and PHPT1) and two histidine
46 kinases (NME1, NME2) have been described (1). We recently reported that murine
47 and human hepatocellular carcinomas (HCCs) exhibit elevated histidine
48 phosphorylation and decreased levels of the histidine phosphatase LHPP. Re-
49 introduction of LHPP resulted in decreased pHis levels in vitro and prevented tumor
50 formation in an HCC mouse model, suggesting that elevated pHis is pathological (3).
51 Another recent study showed that LHPP protein expression correlates with survival
52 of colorectal cancer (CRC) patients, again suggesting that LHPP acts as a tumor
53 suppressor (4).

54 Inflammatory bowel disease (IBD) is a major risk factor for CRC (5). IBD is a
55 general term for intestinal disorders characterized by chronic colitis, such as Crohn's
56 disease (CD) and ulcerative colitis (UC). The etiology and the molecular
57 pathophysiology of IBDs are incompletely understood, resulting in insufficient
58 progress in the development of novel therapies (6). Importantly, inhibition or deletion
59 of the K⁺ channel KCa3.1 prevents colitis progression (7), and PGAM5 inhibits
60 KCa3.1 by dephosphorylating NME2-pHis118 (8). Taken together, the above
61 suggests that pHis may play a role in the pathology of IBD.

62

63 **Results and Discussion**

64 To investigate if histidine phosphorylation plays a role in colitis, we analyzed a
65 publicly available transcriptomic profile (E-GEOD-16879) from colon samples of
66 healthy humans and treatment-naïve IBD patients (9). Patients suffering from CD or
67 UC showed significantly decreased expression of *LHPP*, but no difference in
68 expression of the other known histidine phosphatase genes *PGAM5* and *PHPT1*
69 (Fig. 1A). Expression of *NME1* and *NME2* was significantly upregulated in patients
70 suffering from IBDs (Fig. 1A). Based on these findings, we hypothesized that
71 elevated pHis, via down-regulation of the histidine phosphatase LHPP and up-
72 regulation of the histidine kinases NME1/2, contributes to disease progression.

73 To examine further a role of pHis in IBD, we induced experimental colitis by
74 treating wild-type mice with dextran sodium sulfate (DSS) (10). Mice exhibited mild
75 colitis-like symptoms, after 2 to 4 days, that developed into severe colitis with 20%
76 bodyweight loss and significantly decreased colon length, as observed after one
77 week of treatment (Fig. 1B). Next, we analyzed expression of known histidine
78 phosphatases and kinases at different timepoints of DSS treatment. The histidine
79 phosphatase LHPP, but no other histidine phosphatase, was significantly down-
80 regulated in the colon of wild-type mice after 4 days of DSS treatment, as
81 determined by immunoblotting (Fig. 1C, D). After one week of treatment, LHPP
82 expression was further reduced, indicating that LHPP expression negatively
83 correlated with colitis severity (Fig. 1C, D). Importantly, immunohistochemistry (IHC)
84 revealed that DSS-dependent down-regulation of LHPP was due mainly to reduced
85 expression in IECs rather than in infiltrating immune cells (Fig. 1E). Expression of the
86 histidine kinases was unchanged in DSS-treated mice (Fig. 1C).

87 We next analyzed histidine phosphorylation in colon samples isolated at
88 different timepoints of DSS treatment. Immunoblot analysis of colon lysates showed
89 significantly up-regulated 1- and 3-pHis levels after 7 days of DSS treatment, but not
90 at earlier timepoints (Fig. 1F-I). In agreement with the IHC results described above,
91 DSS treatment increased pHis exclusively in IECs, not in infiltrating macrophages
92 (F4/80-positive cells), as shown by immunofluorescence staining (Fig. 1J). As we
93 observed down-regulation of LHPP at 4 days of DSS treatment but changes in pHis
94 only after 7 days, i.e., LHPP loss preceded increased pHis, we speculate that loss of
95 LHPP contributes to high levels of pHis and disease progression.

96

97 To obtain insight on the role of LHPP in normal development and in colitis
98 progression, we generated full body LHPP knockout (*Lhpp*^{-/-}) mice using
99 CRSPR/Cas9 (see Materials and Methods). *Lhpp*^{-/-} mice were vital, fertile and
100 indistinguishable from littermate controls. Histological analysis of the colonic mucosa
101 did not reveal significant differences between *Lhpp*^{-/-} and *Lhpp*^{+/+} littermates (Fig.
102 2A). Colons of 1.5-year-old *Lhpp*^{-/-} mice displayed no sign of cancer and/or
103 inflammation, and no changes in proliferation or apoptosis (Fig. 2A). Moreover,
104 immunoblot analysis revealed no significant difference in 1- or 3-pHis levels in large
105 intestine lysates of *Lhpp*^{-/-} and *Lhpp*^{+/+} littermates (Fig. 2B, C). Colon from *Lhpp*^{-/-}
106 mice did not display any differences in PHPT1, NME1 and NME2 protein levels (Fig.

107 2B, D), but did exhibit elevated PGAM5 expression, possible as a compensatory
108 mechanism for loss of LHPP (Fig. 2B).

109 To determine whether loss of LHPP has an impact on colitis progression, we
110 treated *Lhpp*^{-/-} and *Lhpp*^{+/+} littermates with DSS. All colitis-related parameters such
111 as weight loss, colon shrinkage, and elevated spleen weight were similar in *Lhpp*^{-/-}
112 and *Lhpp*^{+/+} mice, indicating that LHPP loss does not impact colitis development
113 (Figs. 2E, F). Finally, we did not detect genotype-dependent changes in intestinal 1-
114 and 3-pHis levels after DSS treatment (Fig. 2G, H), or differences in expression of
115 known histidine phosphatases or kinases (Fig. 2I).

116

117 In summary, we show that LHPP loss and increased histidine phosphorylation in
118 intestinal cells correlate with colitis. However, LHPP loss does not appear to be
119 sufficient for either the observed increase in pHis or inflammation, at least in mice.
120 Increased NME1/2 expression or activity, which we observed in IBD patients but not
121 in *Lhpp*^{-/-} mice, might be required in addition to loss of LHPP. Little is known about
122 the role of pHis in inflammation. Fuhs et al reported that both malignant epithelial
123 cells and macrophages show high pHis levels in vitro, and suggested that pHis is
124 important in phagocytosis (2). As activated macrophages are key players in colitis
125 (11), we originally expected that the high pHis levels we observed in our
126 experimental system would be in immune cells. However, results from our IF staining
127 indicate that DSS treatment triggers pHis in IECs. As we observed high pHis levels
128 only in late-stage colitis, we cannot exclude that IECs up-regulate pHis as a
129 response to infiltrating immune cells. Alternatively, upregulated pHis levels in
130 epithelial cells might promote inflammation by inducing the production of pro-
131 inflammatory signaling molecules and recruitment of macrophages. It remains to be
132 determined whether increased pHis is a consequence or a cause of inflammation in
133 IBD. It is also necessary to investigate the role of pHis in the complex interplay
134 between IECs and immune cells. Finally, it will be important to identify histidine
135 phosphorylated proteins and to determine their role in inflammatory diseases.

136 **Materials and Methods**

137

138 **Mice**

139 To generate *Lhpp*^{-/-} mice, exon 2 of the mouse *Lhpp* gene was deleted using
140 CRISPR/Cas9-mediated non-homologous end joining (NHEJ). Two gRNAs were
141 designed to target the *Lhpp* introns 1 (IVS1) and 2 (IVS2). The sequences targeting
142 the respective introns IVS1-catctgactcacatcatgtgagg and IVS2-
143 gcatcctgaagctagccttgagg were selected for optimal on target activity using the
144 CRISPOR online tool (12). NHEJ events at the gRNA target sites led to the excision
145 of the genomic fragment containing exon 2 resulting in a *Lhpp*-null allele.
146 CRISPR/Cas9-mediated modification of the *Lhpp* sequence was carried out by
147 electroporation of fertilized mouse oocytes as previously described (13). *Lhpp*^{-/-} and
148 *Lhpp*^{+/+} mice were maintained in a C57BL/6J genetic background.
149 C57BL/6J wild-type mice were purchased from Janvier Labs. Experimental colitis
150 was induced in 8- to 12-week-old male mice by administering 2.5% DSS in drinking
151 water for up to 7 days according to published protocols (10). All animal experiments
152 conducted were compliant with federal laws and guidelines and were approved by
153 the veterinary office of Basel-Stadt.

154

155 **Histology**

156 Immunohistochemistry (IHC) and H&E stainings were performed as previously
157 described (14). The following primary antibodies were used: cleaved Caspase 3
158 (9664; CST), Ki-67 (12202; CST), LHPP (NBP1-83272; Novus). For
159 Immunofluorescence (IF) stainings, colons were flushed with ice cold PBS (pH 8.5),
160 cryo-fixed in OCT and stored at -80°C. To prevent heat- and acid-mediated pHis
161 degradation, all steps during the IF staining process were performed at 4°C and the
162 pH of all buffers was adjusted to 8.5. After cutting, colon cryo-sections (10µm) were
163 fixed for 1h in 4% PFA, washed with 1x PBS, blocked for 1h using blocking buffer (1x
164 PBS, 1% BSA, 0.05% Triton-X 100) and subsequently incubated O/N with primary
165 antibodies (3-pHis: rabbit, SC44-1 and F4/80: rat, ab6640; abcam) diluted in blocking
166 buffer. Afterwards, slides were rinsed with PBS and incubated for 1h with secondary
167 antibodies (Alexa Fluor 488 anti-rabbit and Alexa Fluor 568 anti-rat; Invitrogen) and
168 DAPI (4083; CST). Finally, the stained sections were washed and mounted with
169 water-based mounting medium (H-1400; Vector Laboratories).

170

171 **Immunoblotting**

172 Immunoblots were performed and quantified as previously described (3). To detect
173 pHis, the following monoclonal primary antibodies were used: 1-pHis (0.5ug/ml, SC1-
174 1), 3-pHis (0.5ug/ml, SC44-1). For regular immunoblot analysis the following primary
175 antibodies were used: Calnexin (ADI-SPA-860; Enzo), LHPP (15759-1-AP;
176 Proteintech), NME1 (3345; CST), NME2 (ab60602; abcam) PGAM5 (ab126534;
177 abcam), PHPT1 (LS-C192376; LSBio).

178

179 **Analysis of publicly available transcriptomic dataset**

180 For mRNA expression analysis the Affymetrix GeneChip Human Genome U133 Plus
181 2.0 gene expression datasets E-GSE16879 (9) was downloaded from ArrayExpress.
182 The probes were matched with gene names, using biomaRt R package. Afterwards,
183 the gene expression levels of *LHPP*, *PGAM5*, *PHPT1* *NME1* and *NME2* were
184 analyzed between different conditions (CTRL, UC, CD).

185

186 **Statistical analysis**

187 Data analysis was performed with PRISM 8.0 (GraphPad). Single comparisons were
188 performed by unpaired, 2-tailed students t-test. Comparison of multiple groups were
189 performed by one-way ANOVA followed by Tukey's post hoc test for multiple
190 comparison. Data are shown as mean \pm SEM. * $P < 0.05$, ** $P < 0.01$, *** $P < 0.001$,
191 **** $P < 0.001$.

192

193 **Author Contributions**

194 M.L. and M.N.H. conceived and designed research; M.L., V.K., D.L. and S.P.
195 performed research; M.N.H. contributed resources and secured funding; M.L., V.K.,
196 D.L., S.P. and M.N.H. analyzed data; and M.L. and M.N.H. wrote the paper.

197

198 **Acknowledgments**

199 This work was supported by an EMBO long-term fellowship to M.L., and by grants
200 from the Swiss National Science Foundation and the European Research Council
201 (MERiC) to M.N.H.

202 **Figure Legends**

203 **Figure 1.** Intestinal inflammation correlates with down-regulation of LHPP and
204 increased histidine phosphorylation. (A) Analysis of publicly available dataset
205 comparing mRNA expression of known histidine phosphatases (*LHPP*, *PGAM5*,
206 *PHPT1*) and histidine kinases (*NME1/2*) in colon tissue from healthy patients (CTRL)
207 with patients suffering from ulcerative colitis (UC) and Crohn's disease (CD). (B)
208 Bodyweight and colon length of mice treated (DSS) and untreated (CTRL) with DSS
209 at indicated timepoints (days). (C) Immunoblot analysis of histidine phosphatases
210 and kinases in colon lysates of DSS-treated and -untreated mice at indicated
211 timepoints. (D) Quantification of LHPP protein levels normalized to Calnexin at
212 different timepoints of DSS treatment. (E) Immunohistochemistry visualization of
213 LHPP in colon samples of mice treated (DSS) and untreated (CTRL) for 7 days with
214 DSS. Scale bar: 100µm. (F-H) Immunoblot analysis of 1- and 3-pHis levels in colon
215 samples from DSS-treated (DSS) and -untreated (CTRL) mice at indicated
216 timepoints. (I) Quantification of 1- and 3-pHis levels in *H*. (J) DAPI and
217 Immunofluorescence staining of colon samples from untreated (CTRL) and 7-day,
218 DSS-treated mice. Scale bars: 50µm (low magnification) and 10µm (high
219 magnification).
220

221 **Figure 2.** LHPP is dispensable for colitis development. (A) IHC and H&E stainings of
222 colon samples of 1.5-year-old *Lhpp*^{+/+} and *Lhpp*^{-/-} mice. Red arrowheads indicate
223 cleaved (cl.) caspase 3 positive cells. Scale bars: 100µm. (B) Immunoblot analysis of
224 1- and 3-pHis and histidine phosphatase protein levels in colon samples from *Lhpp*^{+/+}
225 and *Lhpp*^{-/-} mice. (C) Quantification of 1- and 3-pHis levels in B. (D) Immunoblot
226 analysis of NME1, NME2 and LHPP in colon samples from *Lhpp*^{+/+} and *Lhpp*^{-/-} mice.
227 (E) Bodyweight during DSS treatment. (F) Colon length and spleen weight after 7
228 days of DSS treatment. (G) Immunoblot analysis of 1- and 3-pHis and histidine
229 phosphatase protein levels in colon samples from *Lhpp*^{+/+} and *Lhpp*^{-/-} mice treated
230 with DSS for 7 days. (H) Quantification of 1- and 3-pHis levels in G with n=6. (I)
231 Immunoblot analysis of histidine phosphatases and kinases in colon samples *Lhpp*^{+/+}
232 and *Lhpp*^{-/-} mice treated with DSS for 7 days.
233

234 **References**

235

- 236 1. Fuhs SR & Hunter T (2017) pHisphorylation: the emergence of histidine
237 phosphorylation as a reversible regulatory modification. *Curr Opin Cell Biol*
238 45:8-16.
- 239 2. Fuhs SR, *et al.* (2015) Monoclonal 1- and 3-Phosphohistidine Antibodies: New
240 Tools to Study Histidine Phosphorylation. *Cell* 162(1):198-210.
- 241 3. Hindupur SK, *et al.* (2018) The protein histidine phosphatase LHPP is a
242 tumour suppressor. *Nature* 555(7698):678-682.
- 243 4. Hou B, *et al.* (2020) Tumor suppressor LHPP regulates the proliferation of
244 colorectal cancer cells via the PI3K/AKT pathway. *Oncol Rep* 43(2):536-548.
- 245 5. Choi CR, Bakir IA, Hart AL, & Graham TA (2017) Clonal evolution of
246 colorectal cancer in IBD. *Nat Rev Gastroenterol Hepatol* 14(4):218-229.
- 247 6. de Souza HSP, Fiocchi C, & Iliopoulos D (2017) The IBD interactome: an
248 integrated view of aetiology, pathogenesis and therapy. *Nat Rev*
249 *Gastroenterol Hepatol* 14(12):739-749.
- 250 7. Di L, *et al.* (2010) Inhibition of the K⁺ channel KCa3.1 ameliorates T cell-
251 mediated colitis. *Proc Natl Acad Sci U S A* 107(4):1541-1546.
- 252 8. Panda S, *et al.* (2016) Identification of PGAM5 as a Mammalian Protein
253 Histidine Phosphatase that Plays a Central Role to Negatively Regulate
254 CD4(+) T Cells. *Mol Cell* 63(3):457-469.
- 255 9. Arijis I, *et al.* (2009) Mucosal gene expression of antimicrobial peptides in
256 inflammatory bowel disease before and after first infliximab treatment. *PLoS*
257 *One* 4(11):e7984.
- 258 10. Wirtz S, *et al.* (2017) Chemically induced mouse models of acute and chronic
259 intestinal inflammation. *Nat Protoc* 12(7):1295-1309.
- 260 11. Cader MZ & Kaser A (2013) Recent advances in inflammatory bowel disease:
261 mucosal immune cells in intestinal inflammation. *Gut* 62(11):1653-1664.
- 262 12. Concordet JP & Haeussler M (2018) CRISPOR: intuitive guide selection for
263 CRISPR/Cas9 genome editing experiments and screens. *Nucleic Acids Res*
264 46(W1):W242-W245.
- 265 13. Wang W, *et al.* (2016) Delivery of Cas9 Protein into Mouse Zygotes through a
266 Series of Electroporation Dramatically Increases the Efficiency of Model
267 Creation. *J Genet Genomics* 43(5):319-327.
- 268 14. Linder M, *et al.* (2018) EGFR is required for FOS-dependent bone tumor
269 development via RSK2/CREB signaling. *EMBO Mol Med* 10(11).

270

Figure 1

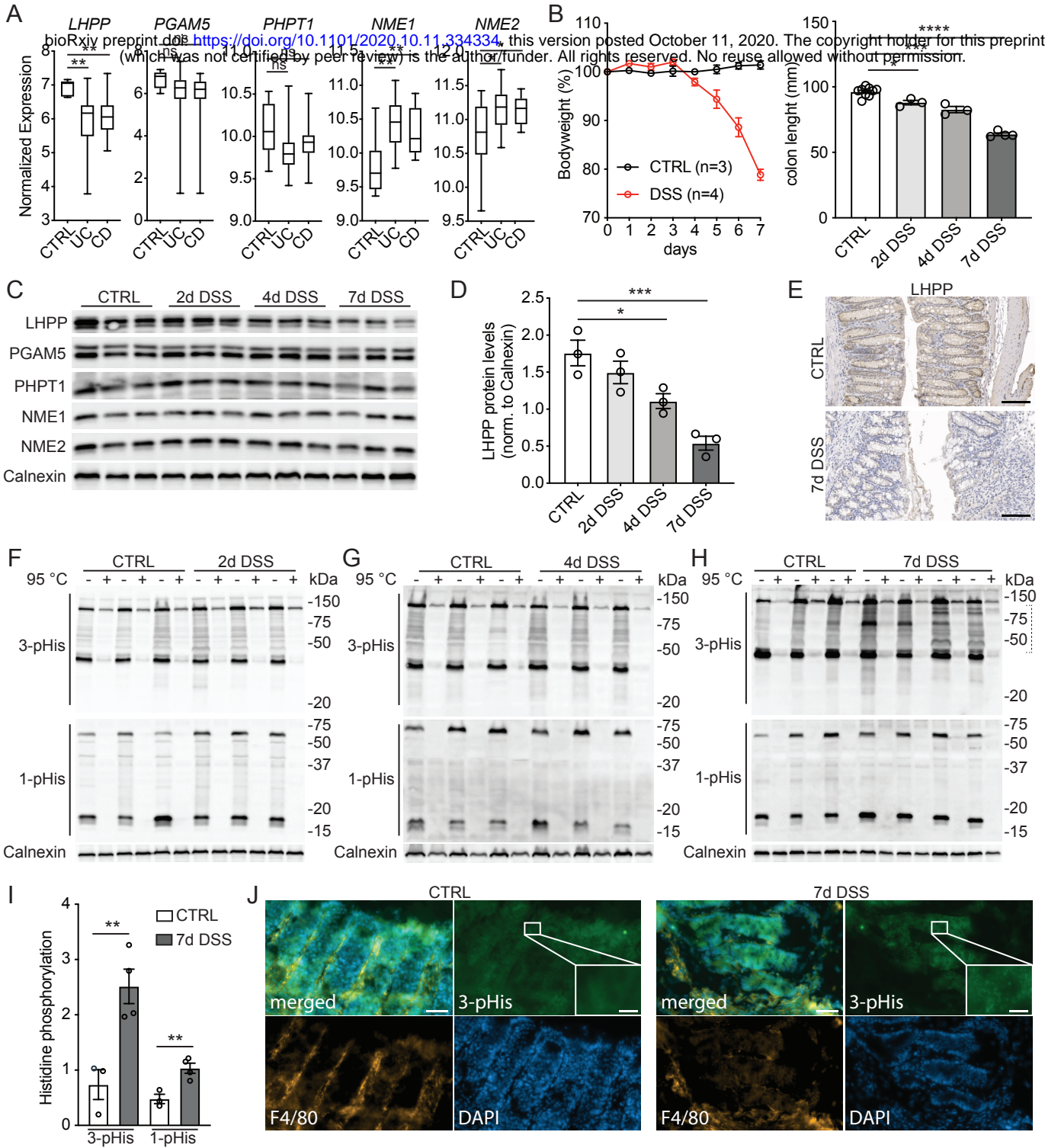


Figure 2

